A Method for Mapping the Turbulence Intensity and Excess Energy Available to Building Mounted Wind Turbines over a UK City

F. C. Emejeamara, A.S. Tomlin*

Energy Research Institute, SCAPE, University of Leeds, Leeds, LS2 9JT, UK

Abstract

Assessing the potential of proposed urban wind installations is further hindered by insufficient assessments of both urban wind resource, and the effectiveness of commercial gust control solutions within built up areas. Evaluating the potential performance of wind turbines within the urban environment requires an estimation of the total energy that would be available to them were effective control systems to be used. This paper presents a methodology for estimating the excess energy content (*EEC*) present in the gusty urban wind, which is usually under represented when using assessments based only on mean wind speeds. The method is developed using high temporal resolution wind measurements from eight potential turbine sites within the urban and suburban environment. By assessing the relationship between turbulence intensities and the *EEC*, an analytical methodology for predicting the total wind energy available at a potential turbine site is proposed. Sensitivity analysis with respect to temporal data resolution on the predicted *EEC* is also demonstrated. The methodology is then integrated with an analytical methodology that was initially developed to predict mean wind speeds at different heights within a UK city based on detailed mapping of its aerodynamic characteristics. Additional estimates of turbulence intensities and *EEC* based on the current methodology allow a more complete assessment of the wind resource available. The methodology is applied to the UK city of Leeds as a case study and the potential to map turbulence intensities and the total kinetic energy available at different heights within a typical urban city is demonstrated.

1.0   Introduction

In the last decade, increased awareness of anthropogenic contributions to climate change, changing economic and regulatory environments, and technological innovations have resulted in renewed interest in decentralised small scale low-carbon energy resources. These distributed energy sources in the form of micro-generation have a number of positive features such as reduction in transmission

losses, reduced dependency on energy imports, increased investment in clean energy technologies, etc. Within cities however, solar installations have developed more rapidly than wind turbines. The perception of low mean wind speeds and relatively high aerodynamic noise levels have been a key concern for power generation through small wind turbines within semi-urban and urban areas. The highly turbulent nature of urban wind is also a concern, and is difficult to assess due to the sparsity of measurements within urban areas. On the other hand, several studies have demonstrated a large untapped potential for wind turbines within cities if appropriately located [1-4].

Small-scale wind turbines can be classed into two major groups: Horizontal Axis Wind Turbines (HAWT) and Vertical Axis Wind Turbines (VAWT). Although HAWT designs have been greatly developed over recent years compared to VAWTs, they are known to suffer higher performance degradation when operating in a fluctuating, turbulent (urban) wind. This may result from increased use of control power in the correction of yaw misalignment error (with a cos^2 dependence on the relative wind angle [5]). A few studies have suggested improved methods of measuring yaw misalignment in HAWTs such as using SOnic Detection and Ranging (sodar) or Light Dectection and Ranging (LiDAR) systems [6, 7]. Although these possess great potential, they face enormous challenges such as cost and sensitivity of both sodar and LiDAR systems for different weather and turbine operating conditions within an urban environment [6, 8]. However, the ability of VAWTs to handle rapid changes in wind direction and to operate at lower tip speed ratios resulting in reduced noise emissions, potentially makes them a good choice of configuration for urban environments. VAWTs are known to suffer from issues such as lower peak efficiencies, low starting torques and narrower operating ranges (i.e. higher cut-in wind speeds). Many of these issues can be addressed by employing effective control algorithms within the turbine system's operations [9, 10]. In addition, a number of studies have assessed the potential of control technologies which are able to track short term changes in wind speeds in order to allow turbines to operate more efficiently within urban areas (gust tracking solutions [11-14]). The complex and gusty urban wind resource is affected to a large extent by the urban surface topography which is strongly influenced by the shape of buildings and structures, building arrangements and densities [15, 16], and even more strongly by building height variability [1, 17]. Hence, in order to achieve improved and effective deployment of small wind systems in urban areas, accurate methods for estimating wind speeds and turbulence, as well as the total (kinetic) energy resource available at potential urban sites must be developed.

Previous studies have shown that it is possible to provide analytical predictions of the mean wind speed over an area as a function of height [18, 19]. This methodology is adopted by the UK Met Office in their small scale wind resource study [20] and involves taking wind speeds from a regional climate and scaling them up to a height at which the frictional effect of the surface is negligible. This

wind speed is then scaled back down whilst accounting for surface roughness effects upon the wind profile. Based on similarity theory [21] a logarithmic profile is used:

$$U = \frac{U_*}{\kappa} \ln\left(\frac{z-d}{z_0}\right) \tag{1}$$

where U is the mean wind speed, U_* is the friction velocity, κ is the Von Karman constant (≈ 0.4), the aerodynamic parameters z_0 and d represent the roughness length and displacement height respectively, and z is the height above the ground. Accurate estimations of the surface aerodynamic parameters have been shown to be critical in applying such a simple method effectively over complex urban surfaces, and various approaches have been developed to improve the accuracy of z_0 and d estimations for urban surfaces based on building features such as frontal and plan area densities and building height variability [15, 22-24]. These methods have been used to provide city wide maps of wind resource potential based on mean wind speeds which provide input to feasibility studies for proposed installations [1].

Urban wind, however, is characterised by strong fluctuations in both wind direction and magnitude as a result of the enhanced local surface roughness. For example, the turbulence intensity at a given hub height within the urban boundary layer has been observed to be twice that of a corresponding rural reference value [25]. On the one hand, without effective controls this enhanced turbulence can tend to decrease the efficiency of the turbine system at converting (kinetic) energy in the wind to electrical or mechanical power. However, on the other hand, enhanced turbulence can increase the total (kinetic) energy available to the wind turbine system [26] thus highlighting the potentially dual influence of local turbulence on wind turbine power output. Cochran [26] suggested the (kinetic) energy available at the turbine hub height can vary by as much as 20% depending on the turbulence level at a given site. Lubitz [27] considered the effect of local turbulence on the power output from a small wind turbine system (Bergey XL.1) operating in a rural environment. Lubitz's observations showed an increase as high as 4% in turbine power output at high turbulence between 4 ms^{-1} and 7 ms^{-1} and a reduced power output (-2%) at low turbulence over the same range of wind speeds. However, Bertenyi *et al.* [12] suggested that relocating a turbine system from a coastal/open sea site to an urban area will result in 60% loss in power output, depending on whether the energy present in the short period fluctuations can be harnessed. Turbine response time is a key issue in the design and application of a turbine system as it influences turbine performance (i.e. how much energy can be extracted) within an urban wind resource [28]. Thus, the ability to react quickly to changes in wind speed may enable the turbine system to capture additional energy associated with turbulence. After carrying out various small VAWT wind tunnel tests within an urban environment, Kooiman and Tullis [29] suggested the shortest representative practical response time to be 10 s. Hence, due to

inertia, it may be difficult for the turbine system to respond to turbulence events with time scales shorter than 10 s. However, results from field trials within urban and rural environments published by James *et al.* [30] suggested a 10% increase in energy extraction at higher turbulent intensities between wind speeds of $5 - 10$ ms^{-1} when a small turbine system with a response time of approximately one second was employed as compared with periods of lower turbulence intensity. Thus, it is essential that the turbine system employed not only copes with, but thrives in this complex urban wind resource. This can be achieved by employing gust tracking solutions in a bid to maximise energy extraction as wind speed fluctuates by keeping the turbine operation within its region of peak aerodynamic efficiency [12]. The uncertainties surrounding the application of the turbine system manufacturer's performance coefficient and tip speed ratio (i.e. C_p- λ) curve at different potential sites as well as the high cost of accurate measurement and observational studies of urban wind give rise to errors that tend to influence turbine controls.

For these reasons, this study develops a methodology to estimate the level of atmospheric turbulence at a given hub height above a complex urban surface based on parameterisations of the surface aerodynamics. We demonstrate that such a method can efficiently quantify the total (kinetic) energy resource available to a proposed turbine system across an urban region. It also allows the investigation of the influence of turbine response time on the energy available to a well-controlled turbine within an urban environment. This will provide potential customers and manufacturers with relevant information to aid decision making for turbine siting within an urban environment, in the performance evaluation of the proposed turbine system, and in assessing the cost effectiveness of prospective turbine control systems at potential urban sites. The methodology may also be relevant to other 'real world' applications such as pollution dispersion modelling and the estimation of wind loading on urban structures.

The methodology consists of three main stages; mean wind speed prediction, turbulence intensity (*T.I.*) prediction and excess energy estimation. Section 2.1 presents a brief introduction to the selected urban measurement sites and data collection and analysis procedures that were used in the development of the methodology. Section 2.2 introduces methods of characterising the *T.I.* and calculating the excess energy content (*EEC*) of the wind within an urban environment. The methodology for calculating the mean wind speed as a function of height within an urban environment is introduced in Section 2.3. In Section 3.1, we then review several models for predicting turbulence intensities available from the literature and evaluate each one using meteorological data from the sites described in 2.1. Using data from four different cities we assess the accuracy of four *T.I.* prediction methodologies. An analytical methodology for predicting *EEC* is then developed in Section 3.2 by assessing its relationship to *T.I.* across the different urban sites. In Section 3.3 we demonstrate the use of the analytical tools for a case study across the city of Leeds, UK by mapping the mean wind speed, *T.I.* and *EEC* over the city. Finally the main conclusions are presented in Section 4.

2.0   Methodology

2.1   Site description and Instrumentation

Whilst there are a number of sources of UK climatology data with varying degrees of temporal and spatial resolution such as the Met office NCIC (National Climate Information Centre) [31, 32] and Numerical Objective Analysis of Boundary Layer (NOABL) database [33], high frequency wind datasets for urban environments are much scarcer, since datasets acquired for weather forecasting purposes tend to be sited in regions of uninterrupted flow. For a more effective urban wind assessment, given the complex nature of the wind resource within an urban environment, specific high resolution wind data measured above roof heights typical of roof-top wind turbines are required. The temporal resolution should be high enough to capture the time-scales of the turbulent motion and hence needs to be in the order of 1 Hz [12, 34]. Such measurements tend therefore to be collected for research purposes rather than for routine forecasting applications. Based on the availability of data, eight high resolution wind datasets obtained from five different cities namely Leeds, Manchester, London, Dublin and Helsinki were selected for this study. Brief descriptions of these sites are provided below.

Leeds Site

The first two wind datasets were collected at a location within the University of Leeds Campus, Leeds, UK. Three dimensional wind speed data was captured using sonic anemometers (Research-Grade Gill Scientific Instruments model R3-50) at a sampling frequency of 10 Hz located at two different mast heights of 6m and 10m, on the top of the Houldsworth building (roof height approximately 24m; Lat.: 53.809963°, Long.: -1.5574005°). Within this study, Unileeds (H1) represents data collected at mast height of 10m, whilst Unileeds (H2) represents data collected at a mast height of 6m above the roof-top.

Manchester Site

The third wind data set was obtained at a sampling frequency of 20 Hz from a sonic anemometer (Gill Windmaster Pro Sonic Anemometer) mounted on a 5 m mast located on the roof-top of the George Kenyon building within the University of Manchester South campus (also known as the Whitworth Meteorological Observatory site with a building height of 49m; Lat.: 53.467371°, Long.: -2.232006°).

London Site

The London city wind data was collected as part of the Dispersion of Air Pollution and its Penetration into the Local Environment (DAPPLE) project [35, 36] using a Gill R3-100 sonic anemometer at a

sampling frequency of 20 Hz and mounted on a Clark mast (mast height approximately 3.5 m) located at the roof-top of the Westminster city council library building (roof height approximately 15 m; Lat.: 51.521082°, Long.: 0.160505°).

Dublin Site

Wind datasets for the Dublin sites were collected at two locations; St. Pius X National (Girls) School located in Terenure, Dublin 6W (Lat.: 53.337767° , Long.: -60.305283°) and Dublin City Council Building in Marrowbone Lane, located in Dublin 8 (Lat.: 53.337767° , Long.: -6.286186°), Ireland. At both sites, wind speed measurements were taken with a Campbell Scientific CSAT3 three dimensional sonic anemometer at a sampling frequency of 10 Hz and a total height of 12m for Dublin (St Pius) and 17m for Dublin (Marrowbone) above ground level (a.g.l.).

Helsinki Site

The wind dataset for Helsinki was collected at two different locations within the city. The first wind dataset, which is referred to as Helsinki (Urban) within this study, was taken from the rooftop of Hotel Torni (Lat.: 60.167803° , Long.: 24.938689°) at a height of 45 m a.g.l. (mast height approximately 2.3m; total building height approximately 42.7m). The second site, SMEAR III (Station for Measuring Ecosystem-Atmosphere Relationships), is located 4 km north-east of the city centre (Lat.: 60.202817°, Long.: 24.961128°). Measurements were taken from a mast at the height of 31 m with the anemometer located on a horizontal boom, 1.3 m south-west from the measurement mast which in this study is referred to as Helsinki (Suburban). At both sites, the wind speed measurements were taken with a Metek USA-1 three dimensional ultrasonic anemometer at a sampling frequency of 10 Hz. The Helsinki (Urban) site is located within a mixed commercial/residential/industrial area characterized by high roughness and impervious urban land use in all directions, while the Helsinki (Suburban) site is located within an extensive residential area with a high vegetation fraction [37, 38].

2.2   Scope of data collected and analysis

The high resolution wind data described in the previous section were collected at the eight sites between the years 2008 and 2011, with a year-long dataset for each site selected for analysis within this study. The sites are considered as potential turbine sites for the purposes of the current analysis based on evaluation of their mean wind speeds. Due to the unavailability of data across the whole period (2008-2011), the datasets selected are not entirely overlapping but this does not compromise the analysis carried out. The longitudinal free-stream wind speed (U) and wind direction upstream of the rotor (θ) are derived from the horizontal wind components, u (x-direction) and v (y-direction) as follows:

$$\theta = \tan^{-1}(v/u) \tag{2}$$

$$U = u \cos \theta + v \sin \theta \tag{3}$$

while the standard deviation of the longitudinal wind speed is given as

$$\sigma = \sqrt{\frac{1}{T} \sum_{i=1}^{T} (U_i - \overline{U})^2} \tag{4}$$

where U_i represents the free-stream wind speed upstream, $\overline{U}$ is the mean wind speed, and T defines the sample time period.

The high resolution wind data, collected from all sites selected in this study, was averaged at a sample frequency of 1 Hz to ensure data consistency between different sites, and to remove very fast transients. It was then parsed into contiguous 10-min bursts (i.e. T = 10 mins), in accordance with the wind energy industry certification standards [39]. In characterising the degree of turbulence within a burst in terms of statistical properties, the standard parameter of turbulence intensity is employed [18] and is defined in Equation 5 as follows:

$$T.I.(\%) = \frac{\sigma}{\overline{U}} \times 100\% \tag{5}$$

The standard deviation of the fluctuating component of the wind speed, as represented in Equation 5, provides a measure of the degree to which the magnitude of the wind is changing during a given burst period. The turbulence intensity for all observation sites presented within this study were obtained using Equation 5. As a result of $T.I.$ sensitivity to averaging time, turbulence intensities obtained within this study were compared for equivalent burst durations. However, there exists extra energy within shorter frequencies in these urban wind conditions which is usually under-reported due to the use of mean wind speed in calculating the wind power over a given period. This can be defined by two parameters; the Gust Energy Coefficient (GEC) and the Excess Energy Content (EEC). The GEC is defined as the ratio of the total integral kinetic energy in the wind over a given period of time to the assumed energy by only considering the mean of the wind speed within the same period [12]:

$$GEC = \frac{\int_0^T U_i{}^3 \, dt}{\overline{U}^3 . T} \tag{6}$$

where T represents the burst period.

The extra energy contained within transient fluctuation about the mean over a given burst period is represented in this paper as EEC (which is closely related to the GEC) and is expressed as a percentage of the total integral energy:

$$EEC(\%) = (GEC - 1) \times 100\% \qquad (7)$$

The values of *EEC* will be sensitive to the length of the burst periods chosen which in this study is 10 mins (i.e. T = 10 mins). From herein, for simplicity we drop the overbar when discussing mean wind speeds.

2.3   Wind Prediction methodology

The wind prediction model developed by Millward-Hopkins *et al.* [24] for mapping mean wind speeds over cities (referred in this study as the MH model) was adopted. Firstly, this model divides the city map into a grid of neighbourhood regions, with aerodynamic parameters for each region subsequently estimated using geometric parameters derived from digital elevation models (DEM) based upon LiDAR data [1] as inputs into a morphological model [23]. The data employed within the LiDAR based DEM, is further processed to remove outlying data points in a bid to improve the predictive accuracy of the MH model as proposed in Ref [24]. Maps of the aerodynamic parameters over the city are calculated on two grids: a coarse uniform grid (of 5 km resolution) is used to represent regional scale (fetch) aerodynamic parameters, while a fine uniform grid (of 250 m resolution) is used to represent the local aerodynamic parameters, with both maps accounting for the aerodynamics of the upwind urban surface as a result of the influence of the incoming wind direction. These aerodynamic parameters were used as inputs in calculating mean wind speeds at different heights over the city.

For the purpose of complete parameterisation of the city's aerodynamics, neighbourhoods with plan area densities (λ_p; defined as the ratio of total roof area to the ground area in a neighbourhood region) within the range of 0.03 – 0.75 use aerodynamic parameters as calculated by the Millward-Hopkins model [15], while the aerodynamic parameters for neighbourhood regions outside this range are selected according to categories such as woodland, low density urban and open terrain as proposed in Ref [24].

The MH model predicts wind speed at a hub height within the city in three different steps:

Step 1: The model takes the long term average wind speed (U_N) from a regional wind climate database available at 10 m as input and scales this up to the urban boundary layer height (z_{UBL}) using a standard logarithmic wind profile:

$$U_{UBL} = U_N \frac{\ln(z_{UBL}/z_{0-ref})}{\ln(10/z_{0-ref})} \qquad (8)$$

where z_{0-ref} is the open country roughness length of 0.14 m.

The regional wind climate is obtained from a relevant climatology dataset such as the Met Office NCIC database [32], or the NOABL database [33] , which provide wind speeds at a given resolution (e.g. 1 km for Met Office NCIC) over the whole of UK and are valid at a height of 10 m above a smooth surface. These data sets represent long term averages of 30 years and 10 years for the NCIC and NOABL data bases respectively.

.

Step 2: The second step involves down-scaling U_{UBL} through the urban boundary layer to the blending height (z_{bl}) using the logarithmic wind profile while considering the flow at z_{bl} to be homogenous [40]. Hence the mean wind speed at z_{bl} is given as:

$$U_{bl} = U_{UBL} \frac{\ln\left(z_{bl} - \frac{d_{fetch}}{z_{0-fetch}}\right)}{\ln\left(z_{UBL} - \frac{d_{fetch}}{z_{0-fetch}}\right)} \qquad (9)$$

z_{bl} is set to be twice the mean building height, while the aerodynamic fetch parameters $z_{0-fetch}$ and d_{fetch} reflect the influence of the incoming wind direction. Taking into account boundary layer growth as a result of the influence of incoming wind direction, the height of z_{UBL} is estimated as a function of the distance from the upwind edge of the city using Elliot's formula [41] as suggested by Millward-Hopkins [24].

Step 3: Given the complex nature of the flow at the lowest region of the urban boundary layer, predicting the wind speed at heights below the blending height is divided into two stages:

    a. For a hub height (z_{hub}) above the mean building height, the wind speed is calculated using local scale aerodynamic parameters d_{local} and $z_{0-local}$ and a logarithmic profile as shown in Equation 10:

$$U_{hub} = U_{bl} \frac{\ln\left(z_{hub} - \frac{d_{local}}{z_{0-local}}\right)}{\ln\left(z_{bl} - \frac{d_{local}}{z_{0-local}}\right)} \qquad (10)$$

    b. For hub heights (z_{hub}) below the mean building height, the wind speed is calculated using an exponential profile while accounting for the influence of height variation upon the wind profile [42]:

$$U_{hub} = U_{hmeff} \exp\left[9.6\lambda_f(1 - \sigma_h/h_{hm-local}) \times (z_{hub}/h_{hmeff} - 1)\right] \qquad (11)$$

where $h_{hm-local}$ is the normal mean building height within each neighbourhood region, σ_h is the standard deviation of the building heights in each local neighbourhood, h_{hmeff} is a modification of $h_{hm-local}$ that takes into account the disproportionate effect of tall buildings upon the wind flow in areas with heterogeneous building heights[15] and U_{hmeff} is the wind speed at h_{hmeff} obtained using Equation 10.

In order to obtain the final average wind speed predictions, a weighted average of the directionally dependent predictions for the eight compass wind directions (N,NE,E,SE,S,SW,W and NW) based upon the temporal frequency of the wind as recorded at a nearby reference station is calculated.

3.0   Results and Discussion

3.1   Turbulence Intensity ($T.I.$) Prediction Methodology

Comprehensive field studies of atmospheric turbulence over urban environments in general are difficult to achieve and as a result limited in scope. Several studies have used different approaches in characterizing atmospheric turbulence with the two dominant environmental controls on turbulence within an urban environment being the urban heat island [43, 44] and the high roughness of the urban surface (buildings, trees and other large structures) [45, 46]. As a result of the absence of a unifying method for characterizing turbulent transfer within the urban environment, much of the recent work has focused on testing the applicability of different concepts within simplified models in different terrains (several of which are presented in Table 1) and identifying their ranges of applicability. Table 1 lists several approaches proposed by various authors in calculating turbulence intensity for urban locations.

Table 1

Summary of available methodologies used in characterising atmospheric turbulence from previous studies.

No.	Authors	Turbulence Intensity Models
1	Roth [44]	$T.I. = 0.259 + 0.582 \exp(-0.943(z/h_m))$ where $0.8 < z/h_m < 6.3$
2	IEC 61400-1 NTM [47]	$T.I. = T.I._{ref} (a + 1.28\alpha + (b + 1.28\beta)/U)$ where a = 0.75; b = 3.8; $\alpha = 0$; $\beta = 1.4$; $T.I._{ref} = 18\%$
3	ESDU [48]	$T.I. = \dfrac{7.5\eta U_*\left(0.538 + 0.09 \ln\left(\frac{z}{z_o}\right)\right)^p}{\left(1 + 0.156 \ln\left(\frac{U_*}{fz_o}\right)\right)U}$ where $\eta = 1 - 6fz/U_*$, $p = \eta^{16}$, $f =$ Coriolis parameter, $U_* =$ friction velocity
4	DS 472 [49]	$T.I. = 1/\ln(z/z_o)$
5	Ishihara *et al.* [50]	$T.I. = T.I._{ref} (a + 1.28\alpha + (b + 1.28\beta)/U)$ where a = 0.75; b = 3.8; $\alpha = 0.27$; $\beta = 2.7$; $T.I._{ref} = 18\%$
6	Mertens [51]	$T.I. = \dfrac{1}{ln\left\lvert\dfrac{z-d}{z_o}\right\rvert}$

As can be seen from Table 1, three models (3, 4, 6) are based on the local roughness length, two (2, 5) are based on simple corrections related to the mean wind speed, and one (1) is based on the mean building height h_m. Since models 2 and 5 do not contain any representation of the local surface features we do not pursue them further here. From the models presented in Table 1, four were selected and tested at the chosen study sites for their ability to predict $T.I.$ Model 1 proposed by Roth [44] estimates $T.I.$ as a function of h_m and Model 3, proposed by Engineering Science Data Unit (ESDU) in 1985 [48] calculates $T.I.$ as a function of the normalised friction velocity U_* taking into account the surface roughness. Within this study, the frictional velocity is calculated as a function of h_m [44]:

$$U_* = 0.094 + 0.353 \exp(-0.946(z/h_m)) \qquad (12)$$

where h_m is the mean building height in the local neighbourhood.

Model 4 proposed by the Danish Standards [49] estimates $T.I.$ as a function of the roughness length z_o. Mertens [51] however, suggested that ignoring the displacement height (as shown in Model 4) would lead to higher errors in estimating $T.I.$ within a built environment and hence suggested the correction in Model 6. Due to the unavailability of LiDAR data used in the calculation of aerodynamic parameters at some sites, the accuracy of each selected model was tested at four urban sites (Leeds (H1 and H2), Manchester and London) using the measured wind speed data described earlier. However, as is true for all rough surfaces, accurate knowledge of the aerodynamic parameters of an urban environment is necessary to describe and model the turbulence [44]. Hence, the MH model [23, 24] was employed in calculating the aerodynamic parameters over the study area. The turbulence intensity models were tested using two representations of the mean building height parameters; $h_{hm-local}$ and h_{hmeff}. The former is simply the arithmetic average of the building heights in the neighbourhood region, while the latter accounts for the disproportionate effect of taller buildings on the surface drag, as fully described in [15, 24]. Due to the availability of maps of aerodynamic parameters, 4 sites were considered in assessing the validity of the $T.I.$ models.
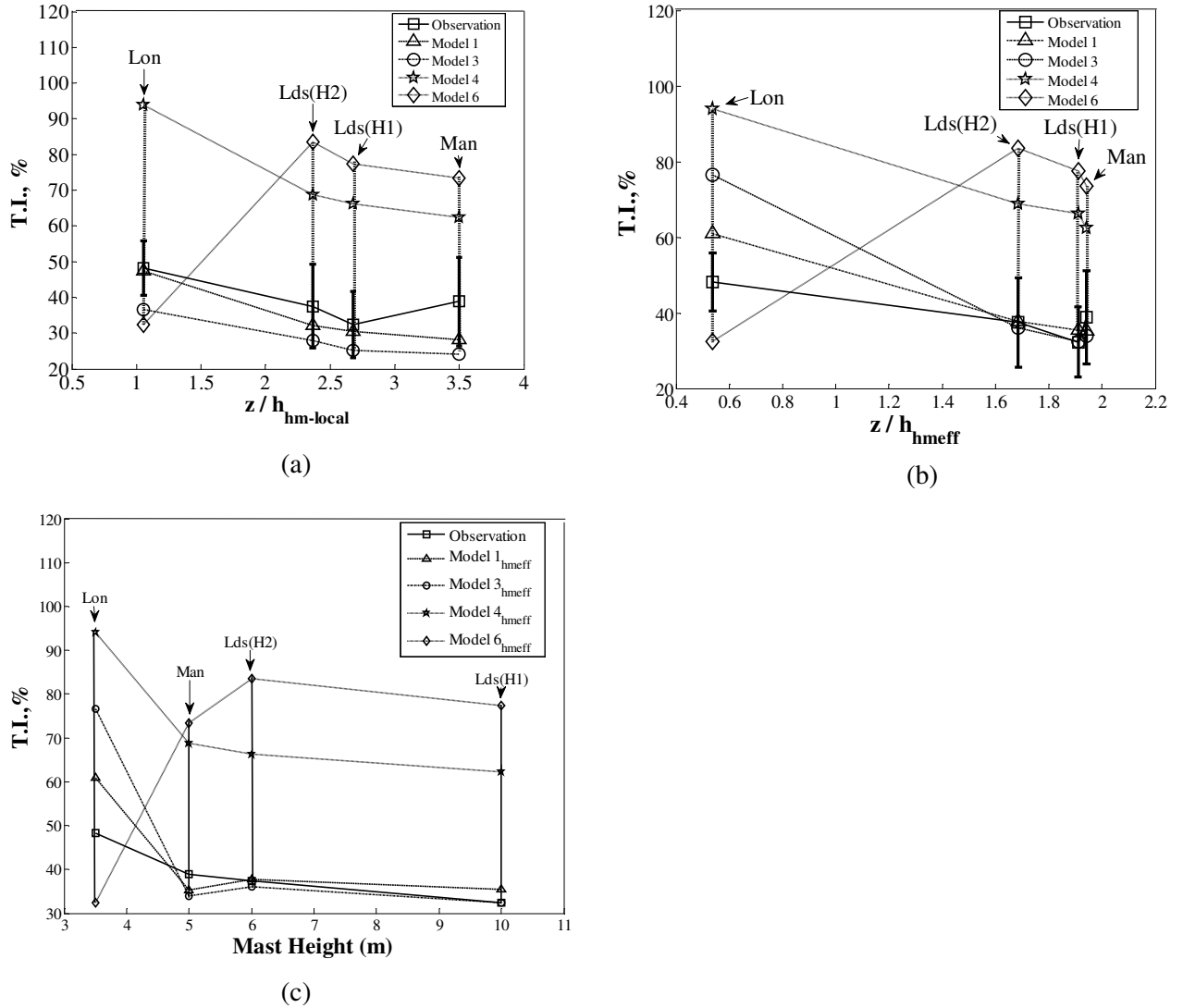
Figure 1: Comparison between four $T.I.$ Models and observations from 4 test sites using (a) local mean building height ($h_{hm-local}$) (b) effective mean building height (h_{hmeff}) (c) Comparing mast heights with $T.I.$ across all test sites. The standard deviation (σ) describing the spread of the measured wind data at the test sites is represented as error bars.

Figure 1 demonstrates the relationship between $T.I.$ and normalised height while comparing results from each model with average $T.I.$ observations obtained from measured wind speed data collected at each test site and a spread of the measured wind data represented by error bars shown in Figure 1. Turbulence intensity observations from measured data show a decrease in $T.I.$ as normalised height increases (i.e. as the observation site moves further away from the ground) with a slight discrepancy in the trend observed at the Manchester site which may be a result of the reduced mast height. A plot of variation of $T.I.$ observations with mast height at each test site (as shown in Figure 1c) shows a reduction in $T.I.$ as the mast height increases thereby highlighting diminishing turbulence levels as

the observations move further away from the roof-top. Unsurprisingly, this supports the idea that higher hub heights for roof mounted turbines would allow them to operate in less turbulent flow regimes.

When using $h_{hm-local}$ as a representation of mean building height, Models 4 and 6 over-predict the turbulence intensities at all test sites except for London where Model 6 under-predicts by 15.87%. Models 1 and 3 substantially under-predict the turbulence intensities at all sites excluding the London and Leeds (H1) sites for Model 1. Substituting $h_{hm-local}$ with h_{hmeff} within each model (i.e. taking into account the disproportionate influence of the taller buildings on surface drag), the results of Models 4 and 6 remain unchanged, whereas Models 1 and 3 reveal significant improvements compared to observations, with both models showing better $T.I.$ predictions at all sites except for the London site which shows an over-prediction of 28.3 % for Model 3 and 12.68% for Model 1. The poor performance of Models 4 and 6 is clearly highlighted in Figure 1 with model results lying outside the fluctuations about the average *T.I.* (represented by the error bars) observed at all test sites. However, when h_{hmeff} was employed, Model 1 and 3 showed improvements at all sites except for London. These aberrant model results at the London site may be a result of z being located near to the roof-top within the urban canopy and also below the displacement height (i.e. $z < d$) where a strong influence of local surrounding structures on the flow properties is observed [36], whereas Model 1 is only expected to be valid at $z/h_{hmeff} > 0.8$ [44].

Studies conducted by Mertens [51] concluded that predicting turbulence intensity within a built environment using the log-law (as employed in Models 4 and 6) will only be valid above a given minimum height (z_{min}). Based on numerous measurements, he proposed z_{min} to be site specific and calculated as:

$$z_{min} = 1.5d \tag{13}$$

where d is the displacement height. Hence, the accuracy of Model 6 at the London site may be greatly affected as a result of the observation site being located below the z_{min} (as shown in Figure 1). A clearer comparison between results from the four models and $T.I.$ observations at all test sites was achieved by using the mean percentage error (*MPE*) as defined in Equation 14 with results presented in Figure 2.

$$MPE(\%) = 100 \times \frac{1}{n}\sum \frac{\left|T.I._{obs} - T.I._{pred}\right|}{T.I._{obs}} \tag{14}$$
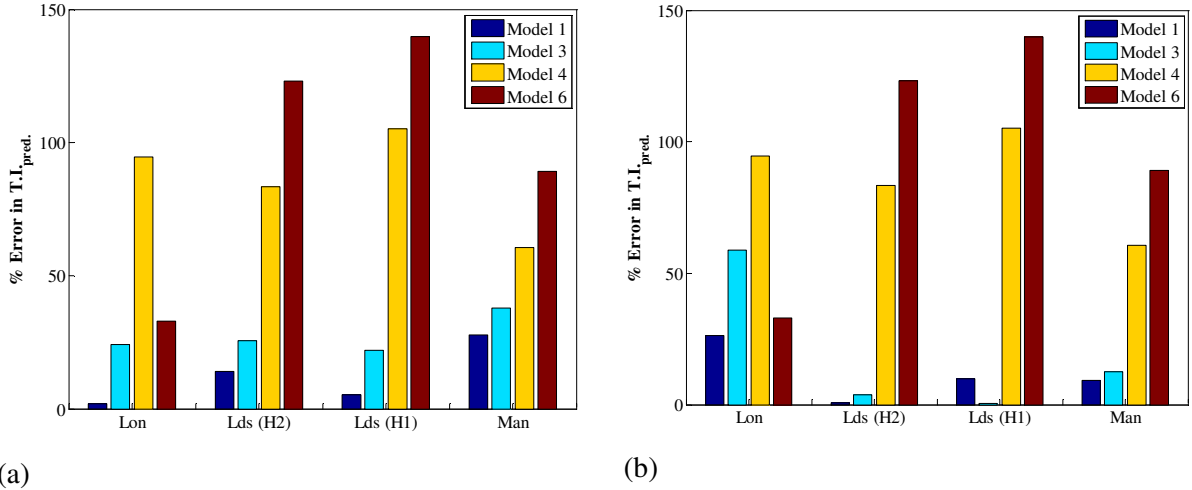
Figure 2: Mean percentage errors for $T.I.$ predictions using Model 1, Model 3 and Model 4 across the 4 test sites when using (a) $h_{hm-local}$ (b) h_{hmeff}

Using the effective mean building height (h_{hmeff}) in Model 1 as demonstrated in Figure 2b resulted in a significant reduction in error in predicting $T.I.$ across all sites except London when compared to using $h_{hm-local}$. A maximum average error of 26% was observed at the London site and a minimum of 0.82% at Leeds (H2). Model 3 (h_{hmeff}) likewise showed lower errors in $T.I.$ prediction when compared to Model 3 ($h_{hm-local}$) at all sites except for London with minimum average error of 0.42% observed at Leeds (H1) and a maximum observed at the London site (58.62%). Models 4 and 6 performed poorly across all sites tested, with average errors above 60% observed at all test sites except for London where Model 6 showed a lower average error of 32.89%. Assessing the overall performance of both building height parameters within each model across all test sites as shown in Figure 3, the use of h_{hmeff} showed better $T.I.$ prediction accuracy and hence was adopted in subsequent analysis. The results also confirm earlier conclusions of Millward Hopkins *et al.* [15, 24], that it is important to take account of building height variability when predicting above roof flow characteristics over complex urban surfaces. Overall Model 1 using h_{hmeff} gave better $T.I.$ predictions compared to Model 3 using h_{hmeff}. Based on these results and the model's simplicity when compared to the complexity involved in modelling frictional velocity below the blending layer height within a built environment, Model 1 using h_{hmeff} was selected within the rest of the study. Testing and validity of such a $T.I.$ model over wider regions will require employing further sets of field measurements from urban sites as well as aerodynamic parameters for each site as they become available.
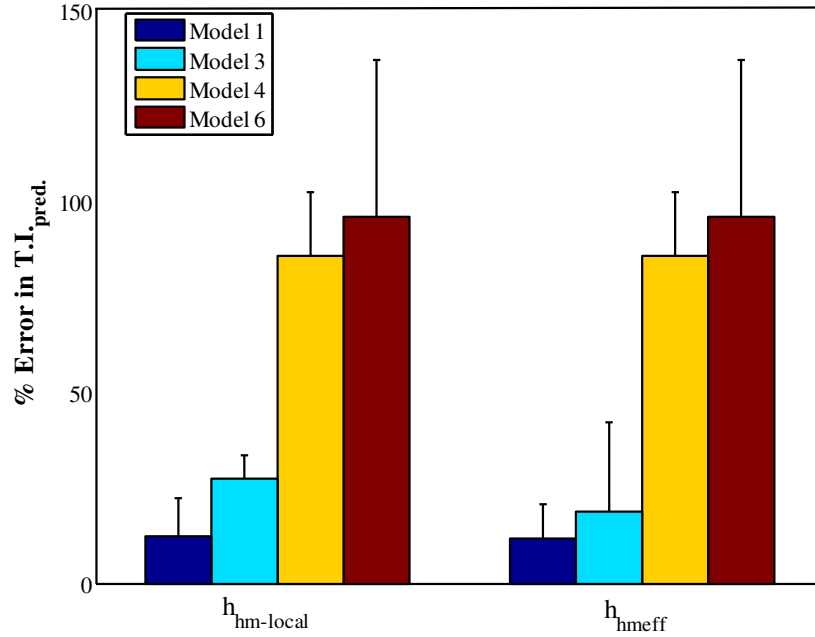
Figure 3: Comparing the mean percentage errors for different models across all test sites when using h_{hmeff} and $h_{hm-local}$. The standard deviation (σ) of the MPE at all test sites is represented by the error bars.

3.2   Excess energy Prediction Methodology

In order to consider the additional energy available at a given hub height within an urban environment, calculated *EEC* values were plotted against the equivalent binned values of $T.I.$ at the 8 urban/suburban potential turbine sites described in section 2. Here, filtering of the raw data was necessary at different averaging times (T_C) of 1 s, 10 s and 60 s resolution in order to mimic different turbine response times, with the burst time assumed to be 10 minutes as explained in Section 2.2. Figure 4 demonstrates a strong relationship between $T.I.$ and *EEC*, with increases in $T.I.$ resulting in increased additional energy available at each site thereby highlighting the potential impact of employing gust tracking solutions within urban environments.
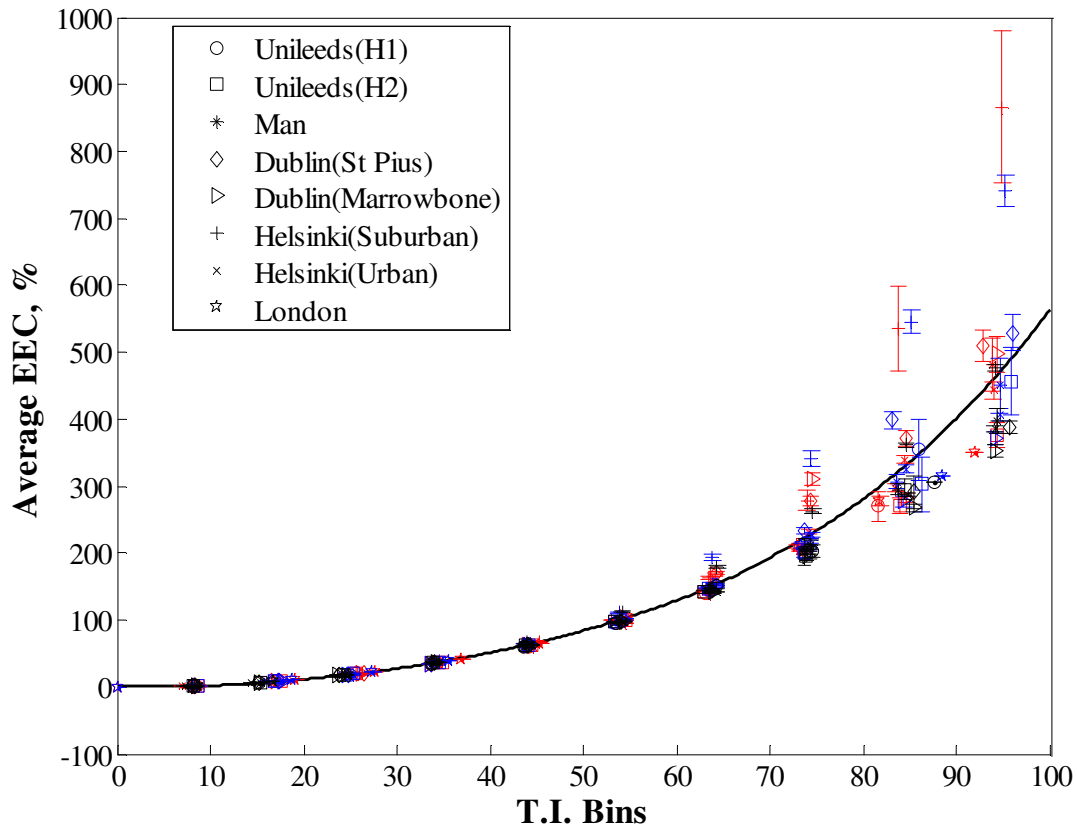
Figure 4: Variation of *EEC* with $T.I.$ at 10mins burst periods for 8 test sites (a) markers represent observations from test sites at different $T_C s$; T_C = 1s (red), T_C = 10s(blue) and T_C = 60s (black) (b) solid line represents empirical fit and the error bars the standard error within each $T.I.$ bin.

As shown in Figure 4, the *EECs* from individual sites lie close to the empirical fit at $T.I.$ values below 60%. The standard error (defined in Equation 17) describing the precision of the *T.I.* averages within each *T.I.* bin is represented by error bars in Figure 4. An increase in scatter observed in *EEC* values as the $T.I.$ increases above 70% across all sites. Whilst the scatter is larger at the $T.I.$ values, this may be a result of the smaller sample sizes within these high turbulence bins as suggested by the error bars. The reliability of the empirical fit is likely to be worse for the high intensity bins but the occurrence of such conditions will be less frequent. For example, even when using 1 s raw data, less than 1% of the data for all sites falls into bins with *T.I.* greater than 70%, whilst less than 7% of mean winds across all sites are less than 1 ms^{-1}. An empirical equation for the prediction of *EEC* values as a function of *T.I.* values was determined using the least square errors approach within MATLAB's best fit tool. A polynomial form was assumed and terms up to 10th order were tested. The lowest errors were determined using a 4th order polynomial and hence *EEC* values are approximated using the following empirical relationship:

$$EEC = 4.2B^4 + 14B^3 + 45B^2 + 99B + 74 \tag{15}$$

where

$B = (T.I.-47)/28$.

$$s_u = \frac{\sigma_i^{EEC}}{\sqrt{N_i}} \tag{16}$$

where σ_i^{EEC} is the standard deviation and N_i the number of data points in the i –th bin.

This suggests that from knowledge of turbulence intensities, the *EEC* available to a particular turbine could be estimated. However, in the above analysis the 1 s raw data resolution assumes that a turbine could respond to changes in wind speed on this short time-scale.

In reality, the turbulence spectrum is both site dependent and averaging time (T_C) dependant and hence the raw data resolution is important when calculating $T.I.$ at a given site. This has critical implications for assessing the *EEC* available to a given turbine, since the filtering time-scale for the raw data should be based on the estimated response time of a particular turbine. Therefore when estimating *EEC*, appropriate data filtering should be carried out prior to the calculation of the $T.I.$ Figure 5 demonstrates the impact of increasing T_C on average *EEC* with increases in T_C resulting in decreasing *EEC* and vice versa. For a given site it is clear that the faster the response time, the greater *EEC* is available to the turbine when compared to the 10 minute mean values with average *EEC* values greater than 18% observed over the 8 sites at a response time of 30s (i.e. T_C = 30s). Up to 80% excess energy is available at a 1 s response time for the most turbulent conditions found close to the roof-top in London. In reality the ability of a turbine and control system to respond on such short time-scales will depend on practical features such as gust tracking control algorithms and power electronics solutions [13, 14, 52]. Thus, it will be interesting in future work to analyse different control methodologies to test whether the predicted excess energy can be realised in practical systems.
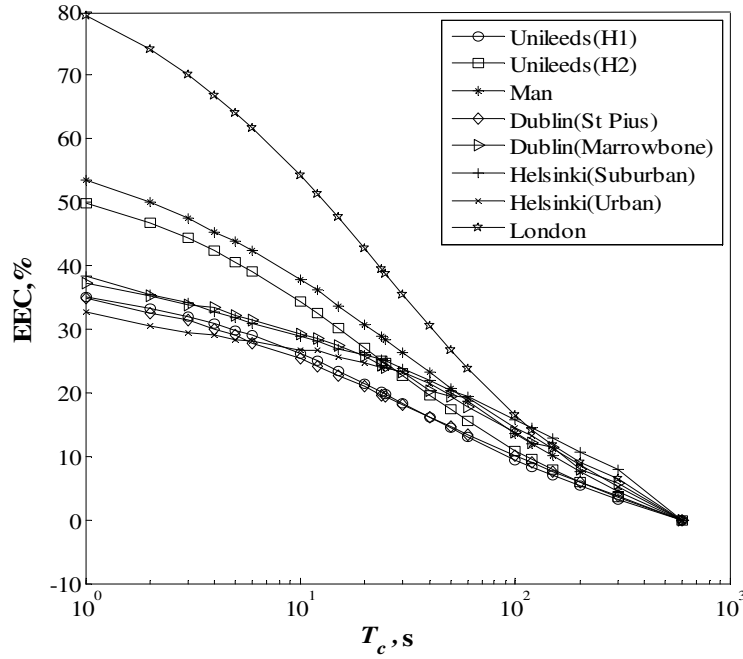
Figure 5: Effect of changes in T_c on average *EEC* at 8 sites highlighting effect of decreasing response time on energy gain

3.3   City scale variations in Wind speed, *T.I.* and *EEC*

In this section we consider the city scale variations of the mean wind speed, *T.I.* and the *EEC*, using the city of Leeds as a case study. Figure 6 shows the mean wind speed over Leeds as predicted by the MH model [24] at 10 m above the local mean building height for each neighbourhood region. Results show an increase in wind speed at this height as the distance increases from the city centre. This suggests that the urban boundary layer is thicker around the city centre as a result of higher surface roughness (see Figure 7). The wind speed map over Leeds, as shown in Figure 6, suggests potential turbine sites across the city with the exception of neighbourhoods within the city centre where the minimum predicted wind speed was observed to be approximately 1.1 ms^{-1}. Further analysis showed that wind speeds at this height (i.e. mean building height) were expected to be low within the city centre due to the presence of tall buildings/structures (as suggested by increased roughness lengths in Figure 7) as well as increased interaction between the local wind and the inherent buildings/structures. However, this may be averted by siting turbine systems above the local maximum building height within the city centre.
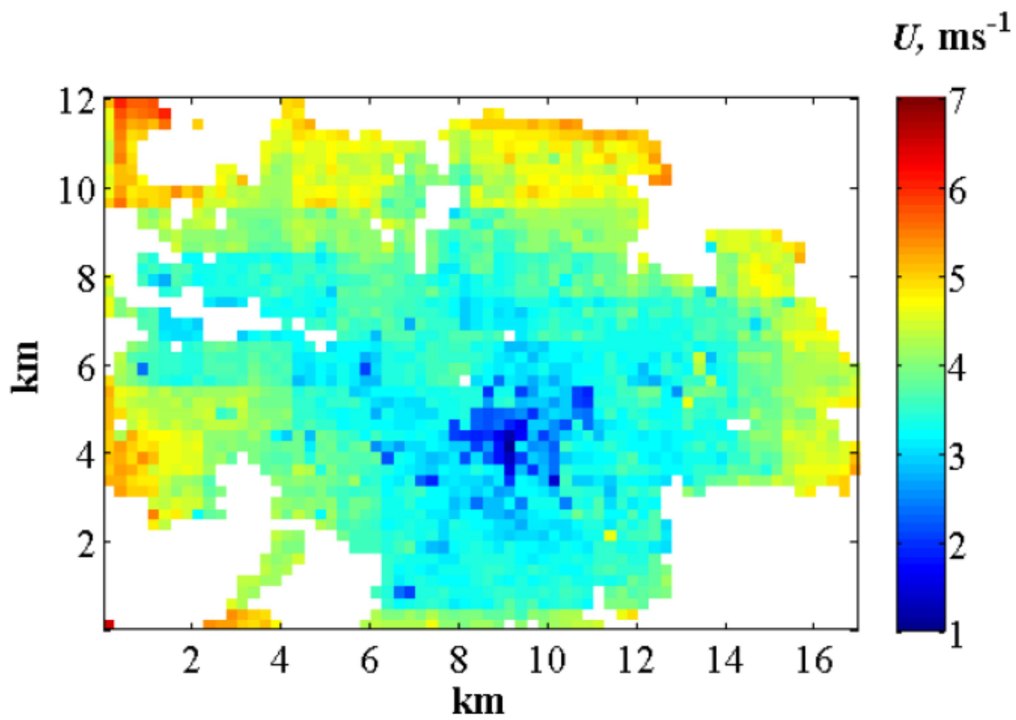
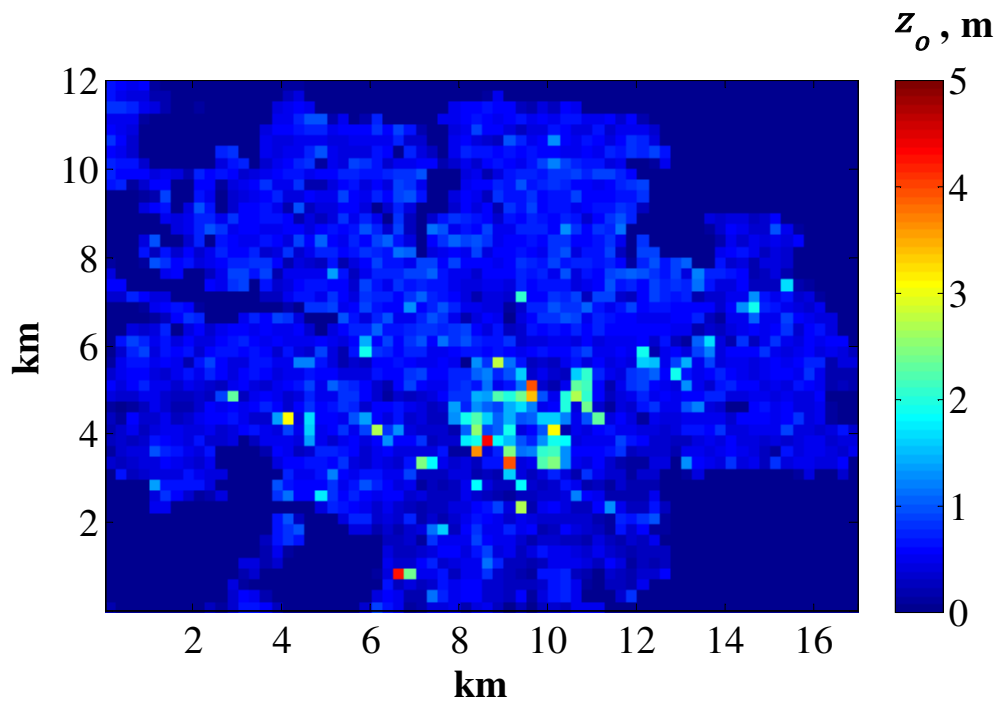**Figure 6:** Predicted mean wind speed (ms^{-1}) at 10m mast height above the mean building heights over Leeds

Figure 7: Predicted surface roughness lengths z_o (m) for the neighbourhoods of Leeds
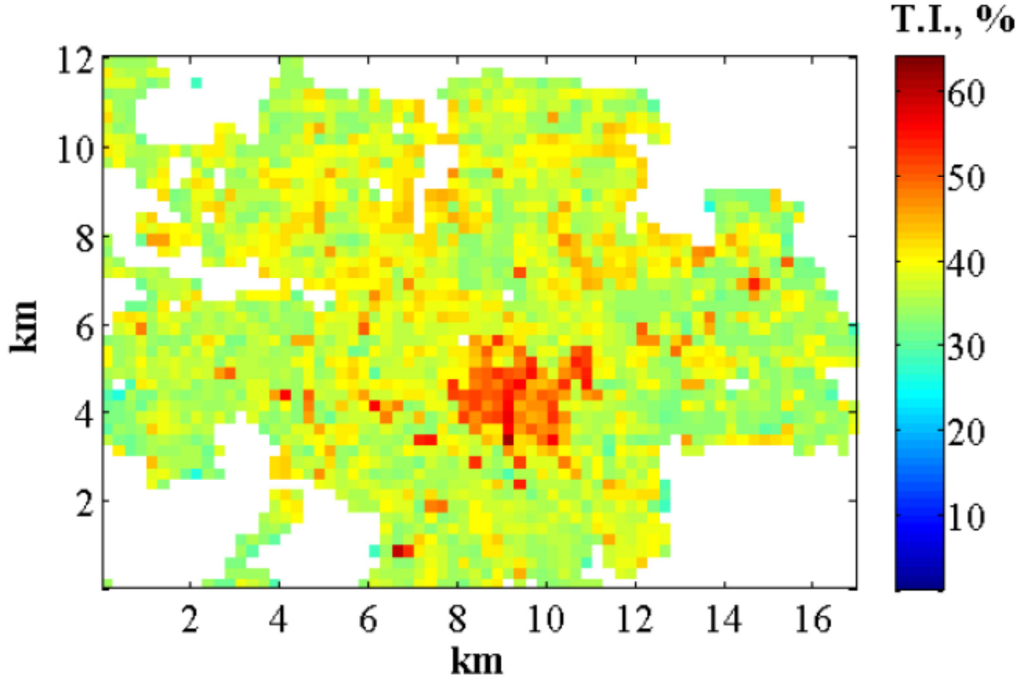
Figure 8: Predicted *T.I.* (%) at 10m mast height above the mean building height over Leeds

Figure 8 shows modelled *T.I.* at a mast height of 10m above h_{hmeff} over Leeds using the methodology proposed in Section 3.1. The map demonstrates high $T.I.$ values at an average of 43% within the built up city centre region, with a decrease in predicted $T.I.$ with increasing distance from the city centre. This suggests increased interaction between incoming flows and complex local buildings and other structures around the city centre and hence is consistent with reduced mean wind speed predictions within the city centre at this height (Figure 6).

Next we mimic the effect of turbine response time by modifying the data filtering time-scale T_C and modelling its effect on the *EEC* available over Leeds. An empirical relationship derived using Matlab software can be established using measured meteorological wind data (as shown in Figure 5):

$$EEC_{T_c} = EEC_{1s} \times \left(1 - \left(\frac{E_{loss}}{100}\right)\right)$$

(17)

EEC_{1s} represents the additional energy available calculated at a turbine response time of 1 s and is obtained using Equation 15, while E_{loss} is the percentage loss in EEC_{1s} with increasing T_C. Based on a "best fit" of the effect of changes in T_C on average *EEC* at all 8 observation sites as shown in Figure

5, E_{loss} was determined to be a 7th order polynomial using the least squares errors approach within MATLAB's best fit tool and is approximated by the empirical relationship:

$$E_{loss} = c_1 M^7 - c_2 M^6 + c_3 M^5 - c_4 M^4 - c_5 M^3 - c_6 M^2 + c_7 M + c_8 \qquad (18)$$

where

$M = (T_c - 80.773)/135.92,$

$c_1 = 37.681$ $c_2 = 233.7$ $c_3 = 379.74$ $c_4 = 121.66$ $c_5 = 75.06$ $c_6 = 2.0584$

$c_7 = 41.493$ $c_8 = 65.304.$

Incorporating Equation 17 into Equation 15, an *EEC* model which accounts for the effect of increasing T_C at 10m above the mean building heights over Leeds city is developed and results presented in Figure 9.
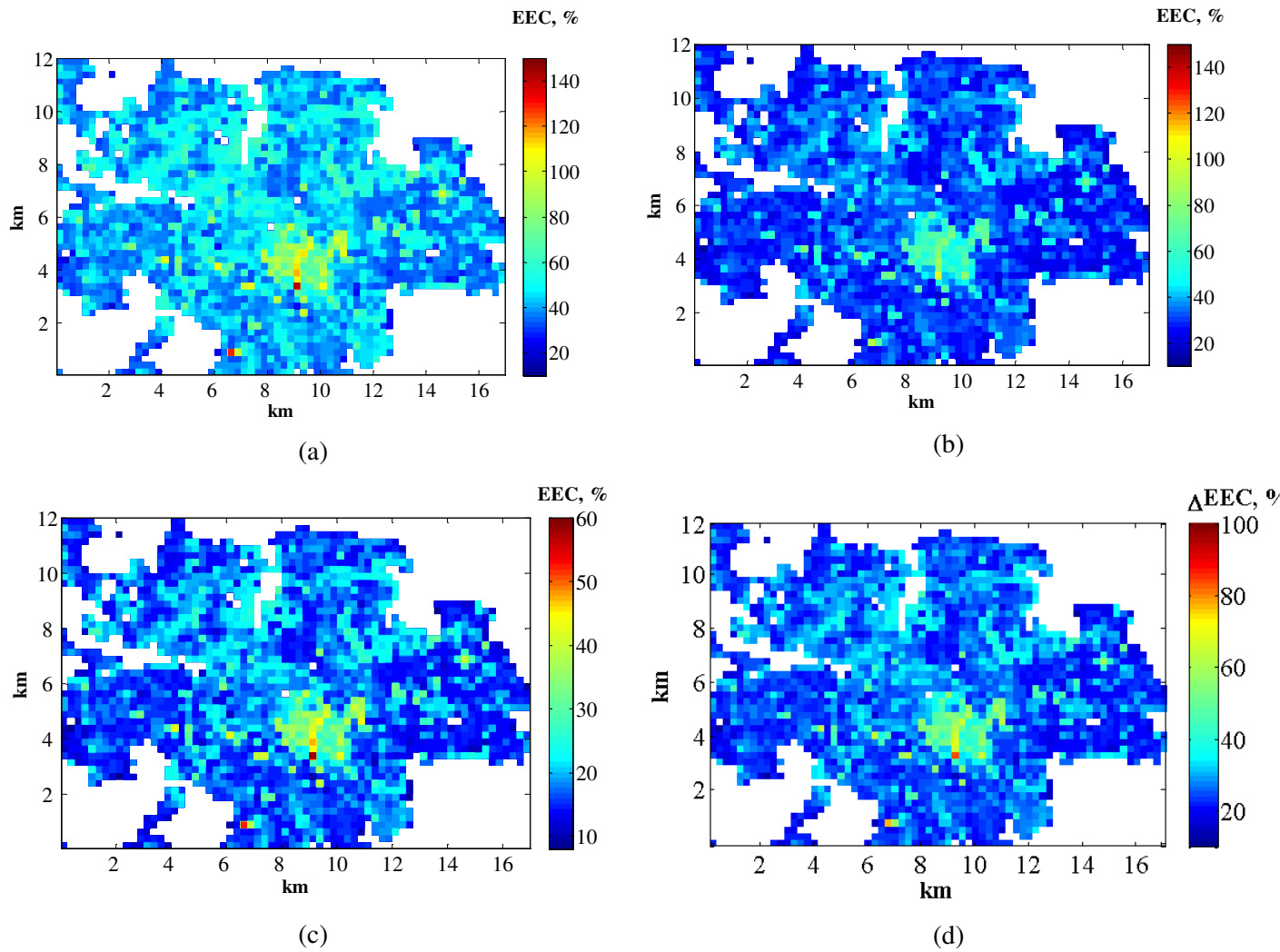
Figure 9: Predicted *EEC* (%) at 10m mast height above the mean building height over Leeds city (a) at T_C = 1s (b) at T_C = 10s (c) at T_C = 60s (d) difference in the predicted *EEC* at T_C = 1s and at T_C = 60s

A map of energy gains at turbine response time of 1 s (i.e. T_C = 1 s [30]) over Leeds is shown in Figure 9a, *EEC* map at response time of 10 s (i.e. T_C = 10 s) which corresponds to the shortest averaging time for anticipated small wind turbine response characteristics suggested in Ref [29] is shown in Figure 9b and *EEC* map at 60 s (i.e. T_C = 60 s; averaging time and subsequent data analysis for wind turbines with rotor diameter less than 16m as described in the relevant standard, IEC 61400 – 12 – 1 (see Annex H) [39]) is shown in Figure 9c. Considering the *EEC* model mapped results over Leeds city (as shown in Figure 9), energy gains at this height were observed to generally decrease with increasing distance from the city centre. This suggests a strong relationship between surface roughness and *EEC* with increasing surface roughness resulting in increasing *EEC* and vice versa. Results showed that increase in T_C from 1 s to 10 s led to a loss in the average *EEC* available from 74.8% to 56.4% around the city centre and 45% to 33.9% over the city. A further 50% loss in average

EEC (i.e. EEC_{10s}) was observed over the city when T_C is increased from 10s to 60s. Figure 9d highlights the difference in *EEC* over Leeds city when T_C is increased from 1s to 60s which highlights. This suggests that employing a well-controlled turbine system with a faster response time might capture the high additional energy available around the city centre. Finally, it is important to point out that although wind speed model results at 10 m above the mean building height show low values around the city centre, *EEC* model results show high energy gains suggesting an effective tracking of the gust by the turbine system could counter the problems of reduced power generation experienced within the urban environment. Additional energy content of a maximum of about 140% is predicted to be available to turbine systems with a fast response time within the city of Leeds at 10 m above the urban canopy. This could potentially be achieved by mounting a well-controlled turbine on top of a tall building (i.e. one which is significantly taller than the local average mean building height).

4.0   Conclusions

The possibility of predicting mean wind speeds, turbulence intensities and excess energy potentially available to turbines employing gust tracking at different heights within an urban environment was demonstrated using analytical down-scaling and *T.I.* estimation methods which employed detailed building data to estimate aerodynamic characteristics over the city. High temporal resolution wind measurements from 8 potential urban rooftop sites were used in developing a model which was able to estimate excess energy content based on the predicted turbulence intensities. Several simplified models for predicting *T.I.* as functions of roughness length, friction velocity and effective mean building height were tested at 4 potential turbine sites. The accuracy of each model was assessed by comparing model predictions with *T.I.* observations from the test sites. Models 4 and 6, based on a simple log function using roughness length, performed poorly at all test sites. Model 1 and Model 3 showed better accuracies for $z/h_{hmeff} > 0.8$ with substantial improvements in performance when the effective mean building height (h_{hmeff}) parameter was used instead of the local mean building height, confirming the importance of building height variability in determining the effect of a complex urban surface on the flow above it. Analysis of measured wind speed data showed increased *EEC* at higher *T.I.* values signifying the potential to estimate the additional energy available to a turbine if accurate modelling of turbulence intensities is achieved. Hence an empirical relationship was derived to predict the *EEC* within a built environment using *T.I.* values obtained at a given turbine response time represented by the appropriate averaging time of the raw data (T_C).

The viability of urban wind energy resource at a city scale was then considered by producing maps of mean wind speed, *T.I.* and *EEC* across the city using Leeds as a case study. Mapped results at a mast height of 10m above the local mean building height over Leeds showed low mean wind speeds of an average of 2.6ms^{-1}, an average turbulence intensity of 46.8% and an average *EEC* of 74.8% within the

city centre area. As the distance from the city centre increased, results showed an increase in the mean wind speed while *T.I.* and *EEC* decreased, thus highlighting the potential of gust tracking solutions in countering problems of reduced turbine power within the built up city centre environment. The effect of increasing turbine response time on *EEC* was also considered. Results showed a decrease in average *EEC* from 74.8% to 56.4% around the city centre and 45% to 33.9% over the city when T_C increased from 1 s to 10 s with a further increase in T_C from 10s to 60s leading to a 50% loss in average *EEC* compared to a response time of 10 s over the city. The results highlight the potential of a fast response turbine system in extracting the additional energy available within the urban environment. Within future work, the study aims at mapping the *T.I.* and *EEC* over more cities that have available LiDAR data as well as analysing different control methodologies to test whether the predicted excess energy can be realised within practical systems.

References

[1]   Millward-Hopkins JT, Tomlin AS, Ma L, Ingham D, Pourkashanian M. Assessing the potential of urban wind energy in a major UK city using an analytical model. *Renewable Energy*, 2013, **60**, pp.701-710.

[2]   Sunderland KM, Mills G, Conlon MF. Estimating the wind resource in an urban area: A case study of micro-wind generation potential in Dublin, Ireland. *Journal of Wind Engineering and Industrial Aerodynamics*, 2013, **118**, pp.44-53.

[3]   Sunderland K, Woolmington T, Blackledge J, Conlon M. Small wind turbines in turbulent (urban) environments: A consideration of normal and Weibull distributions for power prediction. *Journal of Wind Engineering and Industrial Aerodynamics*, 2013, **121**, pp.70-81.

[4]   Drew D, Barlow J, Cockerill T. Estimating the potential yield of small wind turbines in urban areas: A case study for Greater London, UK. *Journal of Wind Engineering and Industrial Aerodynamics*, 2013, **115**, pp.104-111.

[5]   Pedersen T. On wind turbine power performance measurements at inclined airflow. *Wind Energy*, 2004, **7**(3), pp.163-176.

[6]   Harris M, Bryce DJ, Coffey AS, Smith DA, Birkemeyer J, Knopf U. Advance measurement of gusts by laser anemometry. *Journal of Wind Engineering and Industrial Aerodynamics*, 2007, **95**(12), pp.1637-1647.

[7]   Mikkelsen T, Hansen KH, Angelou N, Sjöholm M, Harris M, Hadley P, Scullion R, Ellis G, Vives G. Lidar wind speed measurements from a rotating spinner. *In: 2010 European Wind Energy Conference and Exhibition*, 2010.

[8]   Kragh KA, Hansen MH, Mikkelsen T. Precision and shortcomings of yaw error estimation using spinner-based light detection and ranging. *Wind Energy*, 2013, **16**(3), pp.353-366.

[9]   Aslam Bhutta MM, Hayat N, Farooq AU, Ali Z, Jamil SR, Hussain Z. Vertical axis wind turbine–A review of various configurations and design techniques. *Renewable and Sustainable Energy Reviews*, 2012, **16**(4), pp.1926-1939.

[10]   Danao LA, Eboibi O, Howell R. An experimental investigation into the influence of unsteady wind on the performance of a vertical axis wind turbine. *Applied Energy*, 2013, **107**, pp.403-411.

[11]   McIntosh S, Babinsky H, Bertenyi T. Optimizing the Energy Output of Vertical Axis Wind Turbines for Fluctuating Wind Conditions. *In: 45th AIAA Aerospace Sciences Meeting and Exhibit*.   American Institute of Aeronautics and Astronautics, 2007.

[12]   Bertényi T, Wickins C, McIntosh S. Enhanced energy capture through gust-tracking in the urban wind environment. *In: 48th AIAA Aerospace Sciences Meeting*, Orlando, Florida, USA. 2010.

[13]   Bertenyi T, Young T. Power electronics solutions for Vertical Axis urban wind turbines. *In: Electrical Power & Energy Conference (EPEC)*. IEEE, 2009, pp.1-7.

[14]   Acosta JL, Combe K, Djokic SZ, Hernando-Gil I. Performance assessment of micro and small-scale wind turbines in urban areas. *Systems Journal, IEEE*, 2012, **6**(1), pp.152-163.

[15]   Millward-Hopkins JT, Tomlin AS, Ma L, Ingham D, Pourkashanian M. Aerodynamic Parameters of a UK City Derived from Morphological Data. *Boundary-Layer Meteorology*, 2012, pp.1-22.

[16]   Rafailidis S. Influence of building areal density and roof shape on the wind characteristics above a town. *Boundary-Layer Meteorology*, 1997, **85**(2), pp.255-271.

[17]   Millward-Hopkins JT, Tomlin AS, Ma L, Ingham D, Pourkashanian M. The predictability of above roof wind resource in the urban roughness sublayer. *Wind Energy*, 2012, **15**(2), pp.225-243.

[18]   Burton T, Sharpe D, Jenkins N, Bossanyi E. *Wind Energy Handbook.* John Wiley & Sons Ltd, West Sussex, UK, 2001.

[19]   Manwell JF, McGowan JG, Rogers AL. *Wind Energy Explained: Theory, Design and Application.* Second ed. John Wiley & Sons Ltd, West Sussex, UK, 2002.

[20]   UK Met Office. Small-scale wind energy technical report. Available from: https://www.carbontrust.com/media/85174/small-scale-wind-energy-technical-report.pdf. 2008. [Accessed 20/06/2014].

[21]   Businger JA, Wyngaard JC, Izumi Y, Bradley EF. Flux-profile relationships in the atmospheric surface layer. *Journal of the Atmospheric Sciences*, 1971, **28**(2), pp.181-189.

[22]   Di Sabatino S. A Simple Model for Spatially-averaged Wind Profiles Within and Above an Urban Canopy. *Boundary-Layer Meteorology*, 2008, **127**, pp.131-151.

[23]   Millward-Hopkins JT, Tomlin AS, Ma L, Ingham D, Pourkashanian M. Estimating aerodynamic parameters of urban-like surfaces with heterogeneous building heights. *Boundary-Layer Meteorology*, 2011, **141**(3), pp.443-465.

[24]   Millward-Hopkins J, Tomlin A, Ma L, Ingham D, Pourkashanian M. Mapping the wind resource over UK cities. *Renewable Energy*, 2013, **55**(Complete), pp.202-211.

[25]   Bowne NE, Ball JT. Observational comparison of rural and urban boundary layer turbulence. *Journal of Applied Meteorology*, 1970, **9**(6), pp.862-873.

[26]   Cochran BC. The influence of atmospheric turbulence on the kinetic energy available during small wind turbine power performance testing. *In: IEA Expert Meeting on : Power Performance of Small Wind Turbines not Connected to the Grid*, Soria, Spain. 2002.

[27]   Lubitz WD. Impact of ambient turbulence on performance of a small wind turbine. *Renewable Energy*, 2014, **61**, pp.69-73.

[28]   Scheurich F, Brown RE. Modelling the aerodynamics of vertical-axis wind turbines in unsteady wind conditions. *Wind Energy*, 2013, **16**(1), pp.91-107.

[29]   Kooiman S, Tullis S. Response of a vertical axis wind turbine to time varying wind conditions found within the urban environment. *Wind Engineering*, 2005, **34**(4), pp.389-401.

[30]   James P, Sissons M, Bradford J, Myers L, Bahaj A, Anwar A, Green S. Implications of the UK field trial of building mounted horizontal axis micro-wind turbines. *Energy Policy*, 2010, **38**(10), pp.6130-6144.

[31]   UK Met Office. Small-scale wind energy Technical Report. Available from: www.carbontrust.com/media/85174/small-scale-wind-energy-technical-report.pdf.   2008. [Accessed 7/7/2014].

[32]   UK Met Office. UK Climate Summaries. Available from: http://www.metoffice.gov.uk/climate/uk/. 2013. [Accessed August, 2013].

[33]   NOABL database. Available from: http://www.rensmart.com/Weather/BERR. 2014. [Accessed 09/10/2014].

[34]   Barlow J, Halios C, Lane S, Wood C. Observations of urban boundary layer structure during a strong urban heat island event. *Environmental Fluid Mechanics*, 2014, pp.1-26.

[35] Wood CR, Barlow JF, Belcher SE, Dobre A, Arnold SJ, Balogun AA, Lingard JJ, Smalley RJ, Tate JE, Tomlin AS. Dispersion experiments in central London: the 2007 DAPPLE project. *Bulletin of the American Meteorological Society*, 2009, **90**(7), pp.955-969.

[36] Barlow JF, Dobre A, Smalley R, Arnold S, Tomlin A, Belcher SE. Referencing of street-level flows measured during the DAPPLE 2004 campaign. *Atmospheric Environment*, 2009, **43**(34), pp.5536-5544.

[37] Järvi L, Hannuniemi H, Hussein T, Junninen H, Aalto PP, Hillamo R, Mäkelä T, Keronen P, Siivola E, Vesala T. The urban measurement station SMEAR III: Continuous monitoring of air pollution and surface-atmosphere interactions in Helsinki, Finland. *Boreal environment research*, 2009, **14**, pp.86-109.

[38] Nordbo A, Järvi L, Haapanala S, Moilanen J, Vesala T. Intra-city variation in urban morphology and turbulence structure in Helsinki, Finland. *Boundary-Layer Meteorology*, 2013, **146**(3), pp.469-496.

[39] IEC 61400-12-1. Wind Turbines – Part 12-1 : Power performance measurement of Electricity producing wind turbines. Ed, 2005.

[40] Grimmond CSB, Oke TR. Aerodynamic Properties of Urban Areas Derived From Analysis of Surface Form. *Journal of Applied Meteorology*, 1999, **38**, pp.1262-1292.

[41] Elliott WP. The growth of the atmospheric internal boundary layer. *Transactions, American Geophysical Union*, 1958, **39**, pp.1048-1054.

[42] Jiang D, Jiang W, Liu H, Sun J. Systematic influence of different building spacing, height and layout on mean wind and turbulent characteristics within and over urban building arrays. *Wind and Structures*, 2008, **11**(4), pp.275-289.

[43] Oke T. The heat island of the urban boundary layer: characteristics, causes and effects. *In: Wind Climate in Cities*. Netherlands: Springer, 1995, pp.81-107.

[44] Roth M. Review of atmospheric turbulence over cities. *Quarterly Journal of the Royal Meteorological Society*, 2000, **126**, pp.941–990.

[45] Voogt JA, Oke TR. Complete urban surface temperatures. *Journal of Applied Meteorology*, 1997, **36**(9), pp.1117-1132.

[46] Hamlyn D, Britter R. A numerical study of the flow field and exchange processes within a canopy of urban-type roughness. *Atmospheric Environment*, 2005, **39**(18), pp.3243-3254.

[47] IEC 61400-1. Wind turbines – Part 1: Design requirements. Ed3, 2005.

[48] ESDU. Characteristics of atmospheric turbulence near the ground. Part III: Variations in space and time for strong winds (neutral atmosphere). ESDU 75001, UK. Engineering Sciences Data Unit, 1985.

[49] Danish Standard. Code of practice for loads and safety of wind turbine constructions. DS 472, 1992.

[50]   Ishihara T, Yamaguchi A, Sarwar MW. A Study of the Normal Turbulence Model in IEC 61400-1. *Wind Engineering*, 2012, **36**(6), pp.759-766.

[51]   Mertens S. *Wind energy in the built environment.* Multi Science Publishing Company, 2005.

[52]   Scelba G, Consoli A. Gust tracking capability of small direct-drive wind turbines. *In: Sustainable Energy Technologies (ICSET), 2010 IEEE International Conference*. IEEE, 2010, pp.1-6.